*Malaysian Journal of Chemistry, 2025, Vol. 27(3), 571-583*
(Special Issue: *International Conference on Sustainable Materials and Technologies, ICSMT 2025*)

# Interfacial Bonding and Chemical Stability of Hybrid Ceramic-Reinforced AA6061 Surface Composites Prepared by Friction Stir Processing

**Saravanakumar, S.[1], Satheesh Kumar, S.[2], Chandrasekaran, M.[3], Sivakumar Paramasivam[4], Mohammed Musthaq, M. S.[5] and Prakash, K. B.[3]***

[1]Department of Mechanical Engineering, M.Kumarasamy College of Engineering, Thalavapalayam, Karur, 639113, Tamil Nadu, India
[2]Department of Aeronautical Engineering, Nehru Institute of Technology, Coimbatore – 641105, Tamil Nadu, India
[3]Department of Mechanical Engineering, Bannari Amman Institute of Technology, Sathyamangalam, Erode-638401, Tamil Nadu, India
[4]Engineering Department, Mechanical and Chemical Unit, University of Technology and Applied Sciences Muscat, Sultanate of Oman.
[5]Department of Mechanical Engineering, Al Ameen Engineering College, Erode-638104, Tamil Nadu, India
*Corresponding author (e-mail: kbprakash404@gmail.com)

Aluminium matrix composites (AMCs) were produced using friction stir processing (FSP). The matrix material was aluminium alloy AA6061. As reinforcement particles, various kinds of ceramic particles have been used including $Cu_2O$, $Cr_3C_2$, and BN. AA 6061 surface composites of 50% $Cu_2O$ - 50% $Cr_3C_2$, 50% $Cr_3C_2$ - 50% BN and 50% BN - 50% $Cu_2O$ were effectively produced. Optical microscopy and field emission scanning electron microscopy were used to examine the microstructure. Results showed that the microstructure, hardness, impact strength, and wear test were not significantly affected by the kind of ceramic particle. Regardless of the location, every kind of ceramic particle produced a uniform dispersion and strong interfacial bonding in the stir zone. Nevertheless, AA6061AMC exhibited superior hardness and wear resistance compared to other AMCs produced in this work under the same set of experimental conditions. The observed microstructure is associated with the strengthening mechanisms and the change in the characteristics. The details of fracture mode are further presented.

**Keywords:** FSP; Hardness; SEM Analysis; impact; optical microscope

*Received: February 2025; Accepted: May 2025*

Even though aluminium has only been used commercially for a little more than a century, it is currently the most important nonferrous metal and is ranked second after steel in terms of global quantity and expenditure. It has grown in significance across almost every sector of the global economy, including consumer durables and mechanical equipment [1]. The technical importance of aluminium is attributed to a variety of special and alluring qualities. Its workability, low weight, ability to withstand corrosion, and excellent thermal and electrical conductivity are included [2]. Approximately one-third the weight of steel for a similar volume is aluminium due to its specific gravity of 2.7 whereas steel's is 7.85. Though there are certain applications where a cost per unit volume comparison would be more appropriate, cost per pound comparisons is still frequently used in cost analyses, placing aluminium at a clear disadvantage [3]. The price differential becomes noticeably smaller since one pound of aluminium may make three times as many identical-sized pieces as one pound of steel. From an engineering perspective, aluminium comparatively low modulus of elasticity roughly one-third that of steel is likely its most significant flaw. An aluminium component will deflect three times as much under the same loadings as a steel component with the same design [4-5] as alloying or heat treatment cannot considerably change the modules of elasticity, stiffness must typically be provided by design elements like ribs or corrugations [6-8].

The majority of aluminium is used in alloy form for non-electrical purposes. They still have the benefits of being lightweight, having good conductivity, and being resistant to corrosion, but they are far stronger than pure aluminium. There are currently several alloys that, despite typically being weaker than steel, have tensile qualities that are better than the HSLA structural grades, with the exception of ductility [9]. Designers can often optimize their design and then customize the material to meet their individual needs, as alloys can be up to 30 times stronger than pure aluminium. Although most aluminium alloys have better strength-to-weight ratios than steel and other structural metals, their wear, creep, and fatigue qualities are typically not that good.

†Paper presented at the International Conference on Sustainable Materials and Technologies (ICSMT 2025)

Fatigue failures frequently happen in aluminium because it frequently lacks an endurance limit, even at relatively moderate forces. Since aluminium alloys have a low melting point, they quickly lose strength at higher temperatures and shouldn't be used in situations where service temperatures are significantly higher than 300°F (150°C) [10]. Cost is frequently the deciding factor when choosing between steel and aluminium for a particular component, while the benefits of lighter weight or resistance to corrosion can frequently be used to offset extra costs. When there is a significant demand for light weight, corrosion resistance, low maintenance costs, or excellent thermal or electrical conductivity, aluminium typically takes the place of steel or cast iron. Additionally, the creation of composites may allow for the improvement of particular material qualities like thermal and electrical conductivity [11-12] Aluminium is being used more often in body panels, engine blocks, manifolds, and transmission cases in modern cars since it is lighter and improves fuel efficiency. Aluminium alloys can be divided into two primary classes according to the manufacturing process: wrought alloys and cast alloys [13-15]. Wrought alloys are designed to have favorable forming properties, such as high ductility, low yield strength, excellent fracture resistance, and good strain hardening, because they are formed as solids through plastic deformation [16-18]. Conversely, the low melting point, great fluidity, and appealing as-solidified structures and qualities are appealing characteristics of the cast alloys [19-21]. These attributes are obviously very varied and so are the alloys that are made to full fill them. Because BN is insoluble at high temperatures with nonmetals and related alloys, it was used to strengthen the aluminium matrix [22]. This method combines simplicity, high grain-refinement efficiency, and the capacity to generate large-scale billets with the UFG structure [23-25]. There are now more FSP applications in the automotive industry for the fabrication of battery trays, heat exchangers, and mixed material joints of aluminium and copper for electrical systems due to increased efforts in light weight construction and the growing demand for electric vehicles [26-28].

Researchers have examined the mechanical behaviour of AA5083 reinforced with several reinforcements, including Si3N4, WC, and Al2O3, in recent years [29-30]. Friction Stir Processing (FSP) is used on a variety of aluminium alloys, including 6061, 5052, and 7075. Various studies have explored the reinforcement of aluminum alloys, with different ceramic particulates to enhance their properties. Because of their exceptional mechanical properties which make them appropriate for a range of engineering applications, metal matrix composites (MMCs) have attracted a lot of interest. Numerous writers provided summaries of various studies aimed at improving these alloys through the application of the FSP approach. Their review provides insights and creative suggestions that may direct future research while highlighting the advancements made in the sector [31-32]. As demonstrated in traditional batch systems, the improved interfacial bonding and chemical stability of hybrid ceramic-reinforced surface composites made by friction stir processing are accompanied by increases in production efficiency through set production and FMS integration [33-34]. To fabricate a surface composite that the performance of the components under real-world positions, the FSP method is suggested to use different reinforcements such boron nitrate, copper oxide, and chromium carbide. It is suggested that these concepts be explored as possible possibilities for developing FSP applications in manufacturing industries.

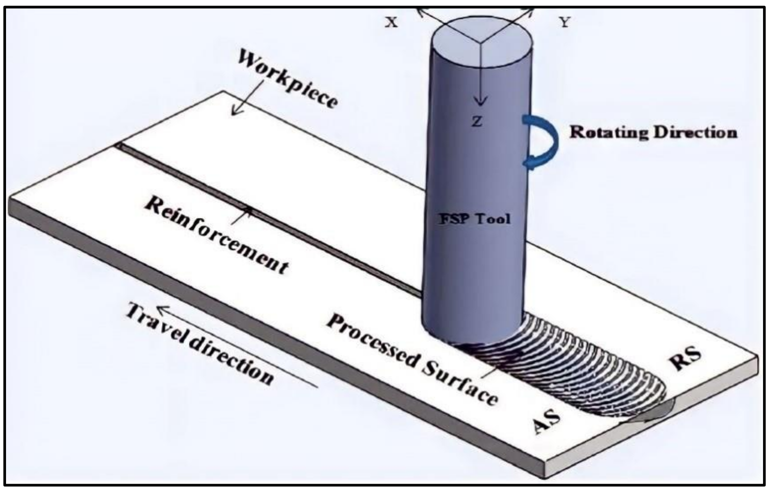


**Figure 1.** Friction Stir Processing.

## MATERIALS AND METHOD

Metals are fabricated through Friction stir Processing (FSP) techniques, by subjected to mechanical deformation and frictional heat without melting in a process called friction stir processing, or FSP. It involves using a spinning device to agitate a solid-state material, which enhances its mechanical properties and smoothness and uniformizes its grain. The material below the melting point of the sheet is softened by heat from the rotating tool's contact with it. Furthermore, the material within the treated zone experiences strong plastic deformation due to the pin's mechanical agitation, which creates a tiny grain microstructure that is dynamically recrystallized. Figure 1 shows a simplified illustration of friction stir processing.

FSP involves complex material movement and plastic deformation. Tool geometry and processing parameters have a significant effect on the temperature distribution and material flow pattern, which in turn influence the microstructural evolution of the material. Tool geometry is the primary factor influencing process development. Tool geometry is critical to material flow and determines the traverse rate at which FSP can be performed. An FSP tool consists of a pin and a shoulder. During the initial phase of the tool plunge, the primary sources of heat are the friction pin and the work piece. Some additional heating results from material deformation. The tool is lowered until the workpiece is in contact with its shoulder. The primary source of heating is the contact between the shoulder and the work piece. The proportions of the pin and shoulder are important from a heating standpoint, but the other design components are not necessary. Process stresses and the homogeneity of microstructure and features are controlled by the tool design. The tool traversal speed (S) along the joint/processing line and the tool rotation rate (N), in either a clockwise or counterclockwise orientation, are two crucial parameters for FSW/FSP. Higher tool rotation rates result in increased friction heating, which boosts temperature and intensifies material swirling and mixing. Process stresses and the homogeneity of microstructure and features are controlled by the tool design. The tool traversal speed (S) along the joint/processing line and the tool rotation rate (N), in either a clockwise or counter clockwise orientation, are two crucial parameters for FSP. Higher tool rotation rates result in increased friction heating, which boosts temperature and intensifies material swirling and mixing. There are numerous uses for friction stir processing, some of which are mentioned here. Microstructural alloy refining in castings. Alteration of a number of characteristics, including wear resistance, corrosion resistance, fatigue, hardness, yield strength, and formability.

### Material Selection

When fabricating composites, the selection of material is the most important factor to take into account. The least expensive material that fulfil the purpose is the best one. The material's suitability for the service circumstances, availability, and maintenance are the aspects taken into account when choosing the material. Physical, chemical, and mechanical properties are critical factors that influence material selection.

Figure 2 shows the aluminium alloy 6061.A commercially available material called AA6061 was chosen. The aluminium alloy in question has a comparatively low strength. Together with strong corrosion resistance, it is renowned for having outstanding process qualities and formability. often used in the manufacturing of chemical equipment and railroad tank wagons; heat treatment cannot solidify it. This article gives the chemical composition of the base alloy as calculated by optical emission spectroscopy.

### Reinforcements of AMMCs

Choosing the right reinforcement is still one of the most important steps in obtaining the greatest qualities from the resulting AMMCs. The inclusion of reinforcement in the AMMCs was chosen because it reduces the pace at which the counter faces wear out and offers protection against thermal shocks, warping at high temperatures, and corrosion under stress. These particles are prone to adhering from the matrix and functioning as abrasive third bodies, which enhances these characteristics.

**Figure 2.** Aluminium Alloy 6061.

**Table 1.** Properties of Boron Nitride.

| **Properties** | **Values** | **Unit** |
|---|---|---|
| Thermal conductivity | 300 | w/m-k |
| Specific heat | 794 | J/kg-k @25 °c |
| Thermal density | 2.25 | g/cc |
| Dielectric constant | 3.9 | - |
| Volume resistivity | 10 | Ohm-cm |
| Young's modulus | 40 | Gpa |
| Knoop hardness | 11 | Kg/mm$^2$ |
| Mohs hardness | < 2 | |

**Boron Nitrate (BN)**

The hexagonal crystalline form, also known as h-BN, α-BN, g-BN, and graphite boron nitride, is the most stable one. The layered structure of hexagonal boron nitride (space group = P63/mmc, point group = D6h) is comparable to that of graphite. Strong covalent connections bind the atoms of boron and nitrogen within each layer, while weak Van der Waals forces hold the layers together. The atoms in these sheets are eclipsed, with boron atoms sitting above nitrogen atoms, therefore their interlayer "registry" is different from the pattern observed in graphite. This registry represents the B-N bonds' polarity.

**Copper Oxide**

A chemical made of copper and oxygen, copper oxide is important in a lot of different industries because of its special qualities and uses. It has the chemical formula $Cu_2O$ and can be found in two different forms: cupric oxide ($Cu_2O$) and cuprous oxide ($Cu_2O$), each with unique properties and uses. The main application of copper oxide is in the semiconductor sector. In particular, cuprous oxide is a p-type semiconductor, which means that its concentration of positive charge carriers is greater than that of negative charge carriers. Because of this characteristic, it is used in the production of rectifiers, diodes, and solar cells. Because of its effective solar energy conversion to electricity, it is used in solar energy harvesting devices, which has aided in the expansion of the renewable energy industry. Additionally, copper oxide is used in catalysis, namely in the oxidation of organic substances.

**Chromium Carbide**

The chemical formula for chromium carbide, $Cr_3C_2$, is a combination of the elements chromium and carbon. It is categorized as a ceramic material and has certain special qualities that add its value to a wide range of industrial uses. High melting point, remarkable hardness, and resistance to oxidation, corrosion, and wear are among of this compound's distinguishing qualities. Chromium carbide's exceptional hardness among the highest of any known material is one of its primary characteristics. The strong covalent connections that form in its lattice structure between the carbon and chromium atoms are responsible for its hardness. Chromium carbide is as frequently employed as a coating material for surfaces that are subjected to abrasive or erosive conditions, such as drill bits, cutting tools.

**FSP Tool Design**

The FSP tool is a crucial and essential component of the procedure. A shoulder and a concentric pin make up the square and cylindrical tools depicted in Fig. The D2 steel material is used to make the tools used in this work. Processing was done using a non-consumable rotating tool composed of HCHCR steel that had been hardened to 53HRC. Square, cylinder-shaped profile was employed to create the surface composite. The tool design is the most important factor in the friction stir processing. In the FSP process, a cylindrical shouldered tool with a central probe is usually utilized. It is rotated, progressively introduced into the work piece, and moved down a line to be left unprocessed. There are three main purposes for the instrument. The work item receives the applied load first. Second, the material that the tool shoulder is covered with softens due to the frictional heat the tool produces. Heat is produced by the plastic deformation of the work piece and the friction that exists between the tool and the work piece. Third, the tool stirs and mixes the material around it. The material flow, heat generation, and working volume are all significantly influenced by the height, shape, and orientation of the probe as well as the shoulder surface's profile and diameter. In the end, these variables affect the agitated zone's microstructure and characteristics.


**Figure 3.** FSP TOOL.

AA6061 plate, measuring 100 mm in length, 50 mm in breadth, and 10 mm in thickness, was the material employed for this investigation. We created a groove in the middle of the specimens containing copper oxide, boron nitride, and chromium carbide particles so that each powder could be scattered throughout. Using a non-consumable tool made of high carbon high chromium steel with a shoulder diameter, cylindrical pin diameter, and length of 25 mm, 6 mm, and 2.7 mm, respectively, the common parameter for all reinforcement with tool rotation speed was 1000 rpm with transverse speed of 20 mm/min and axial load of 10 KN. The utility is displayed in Figure 3. The tool used for FSP is made of HCHCR steel and has a cylindrical profile. It has been oil hardened to 53 HRC.

**Table 2.** Name & Depth of Reinforcement Filled.

| **Sample** | **Chromium Carbide** ($Cr_3C_2$) 50% | **Copper Oxide** ($Cu_2O$) 50% | **Boron Nitride** (BN) 50% |
|---|---|---|---|
| T1 | ✓ | ✓ | |
| T2 | ✓ | | ✓ |
| T3 | | ✓ | ✓ |

**Table 3**. Aluminium Alloy 6061 properties.

| **Elements** | **Properties** |
|---|---|
| Density | 2700 $Kg/m^3$ |
| Melting Point | $600^0C$ |
| Modulus of Elasticity | 69.5Gpa |
| Thermal conductivity | 200 W/m.K |
| Thermal expansion | 23.5 x $10^{-6}$ /K |
| Electrical resistivity | 0.035x$10^{-6}$ Ω.m |

**Table 4.** Various Tool and Parameter.

| S.NO | Rotational Speed RPM | Transverse Speed mm/min | Axial Force kN | Reinforcements (%) |
|---|---|---|---|---|
| 1 | 1000 | 20 | 10 | 50% $Cu_2O$& 50% $Cr_3C_2$ |
| 2 | 1000 | 20 | 10 | 50% $Cr_3C_2$ &50% BN |
| 3 | 1000 | 20 | 10 | 50% BN &50% $Cu_2O$ |


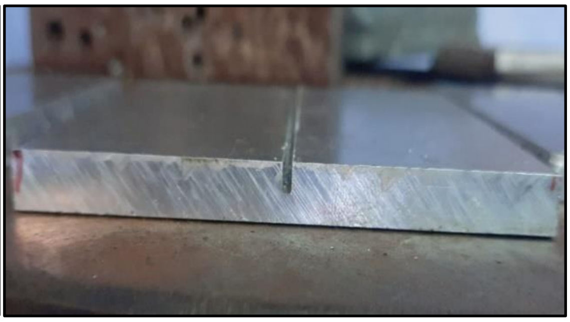

**Figure 4(a)** After grooving of AA6061 test plate **(b)** During FSP on AA 6061 test plate

## RESULT AND DISCUSSION

### Hardness Test

By two passes of FSP, AA 6061 surface composites of 50% $Cu_2O$ and 50% $Cr_3C_2$, 50% $Cr_3C_2$ and 50% BN and 50% BN and 50% $Cu_2O$ were effectively produced. The investigation focused on the impact strength, hardness, and microstructure of the produced surface composite layer, as well as the type of reinforcing particle and FSP passes used. The distribution of the particles in the Aluminium metal matrix with different reinforcement was achieved by a single FSP process, which led to improved hardness and impact strength characteristics in below test grape shown in Figure 5. Test Plate No. 2 (50% Chromium carbide 50% Boron Nitride), which was identified during the hardness experiment, increases the maximum surface hardness. Test Plate 2 consequently displays a higher hardness value is 58 HV in the FSP process. The sample 1 hardness value is 51HV and sample -3 is measured at 52 HV.

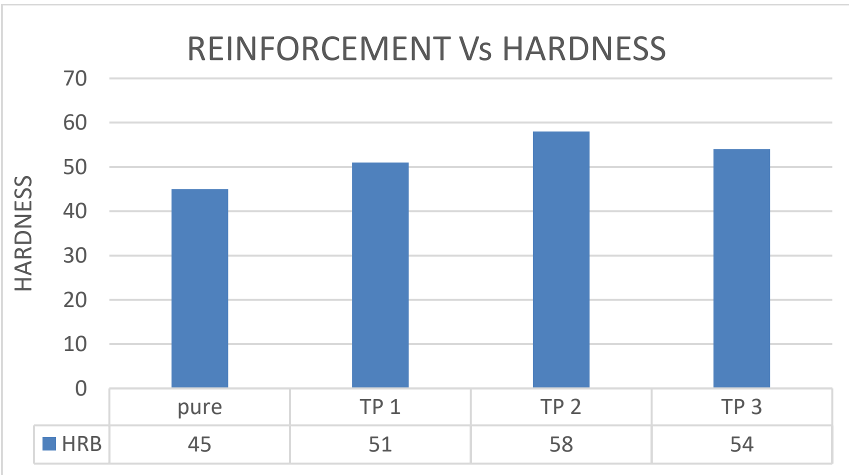


**Figure 5.** Hardness Variation for different reinforcement.

When varying percentages of particles are added, composites with variable reinforcement can be effectively produced. Composites' microhardness is measured, and Figure. 5 displays the findings. As can be shown, the HV of composites rises linearly from 45 to 58 as the number of reinforcing particles increases. Under the same conditions, the maximum HV surpasses 50% Chromium Carbide and 50% Boron Nitride of the aluminium composite value. One physical parameter that shows the ability of a substance to withstand local plastic deformation is its hardness of the reinforcement particles, which serve as reinforcing phases, are distributed throughout the aluminium matrix and limit dislocation migration when plastic deformation takes place. On the other hand, the Orawan mechanism states that particles' ability to control the formation of crystal grains and refine aluminium crystal grains is also responsible for the composite's increased hardness. Because of the greater strengthening effects of dispersion and grain refinement of composites, the composite rises in hardness and crystal grain size as the percentage of chromium carbide and boron nitride increases.

**Impact Test**

An ASTM-recommended technique for assessing impact strength is izod impact strength testing. Usually, impact strength is measured using a sample that has been notched. Impact has a crucial role in determining how long a structure lasts. The sample is broken when the arm strikes it. The impact strength of the sample is calculated from the energy it absorbs. ASTM D256 is the standard for Izod Impact testing in North America. The energy loss per unit of thickness (ft-lb/in or J/cm) at the notch is how the results are expressed. Alternatively, the data could be expressed as the energy loss ($J/m^2$ or $ft\text{-}lb/in^2$) per unit cross-sectional area at the notch. The maximum impact load was achieved of the FSP test plate 2- 36 J and then followed by test plate 1 -16J with 50% $Cu_2O$ & 50% $Cr_3C_2$.

**Wear Test**

The amount of wear on composite and pure aluminium layers. As may be seen, composite wear is less severe than aluminium deposit wear. Figure 6 displays the wear surface morphology of aluminium deposit and composite surface composites of 50% $Cu_2O$, 50% $Cr_3C_2$, 50% $Cr_3C_2$ and 50% BN, and 50% BN and 50% $Cu_2O$ a significant quantity of abrasive particles and particles can be seen on the worn surface in Figures 7 a–d. The worn surface may develop a friction layer as a result of friction, and because the aluminium deposit is less robust and less resistant to cyclic shearing pressure, cracks between the friction layer and base layer may start and spread more easily. Ultimately, a lot of abrasive particles and particles are created when some friction layers are broken and removed from the wear surface. On the other hand, the scattered 50% $Cr_3C_2$ and 50% BN matrix gives the composite a higher hardness and a stronger resistance to shearing strain. Friction layers with a compact structure and high hardness tend to grow on the composite's wear surface, and they have a very strong connection with the foundation layer. Under cyclic shearing strain, the composite's friction layers are difficult to break and can become abrasive dusts and particles. High-hardness friction layers, meanwhile, can lessen further abrasive damage to the base layer. Consequently, the composite shows superior wear resistance and less wear than the aluminium deposit. Figure 6 shows that the worn surface has fewer fractures and abrasive dusts and particles. Additionally, when 50% $Cr_3C_2$ and 50% BN rise, the composite's wear extent lowers because of the improved hardness. For wear resistance, a 50% increase in $Cr_3C_2$ and 50% BN is hence beneficial.

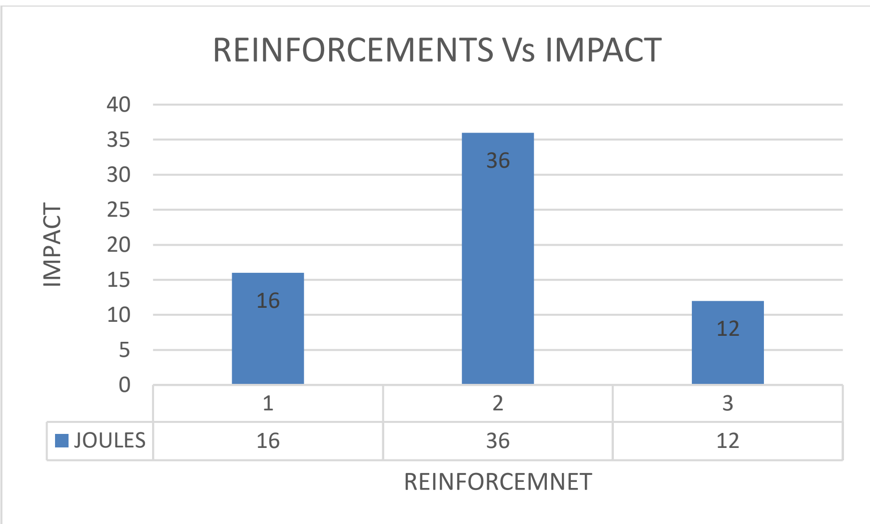


**Figure 6.** Impact Variation.

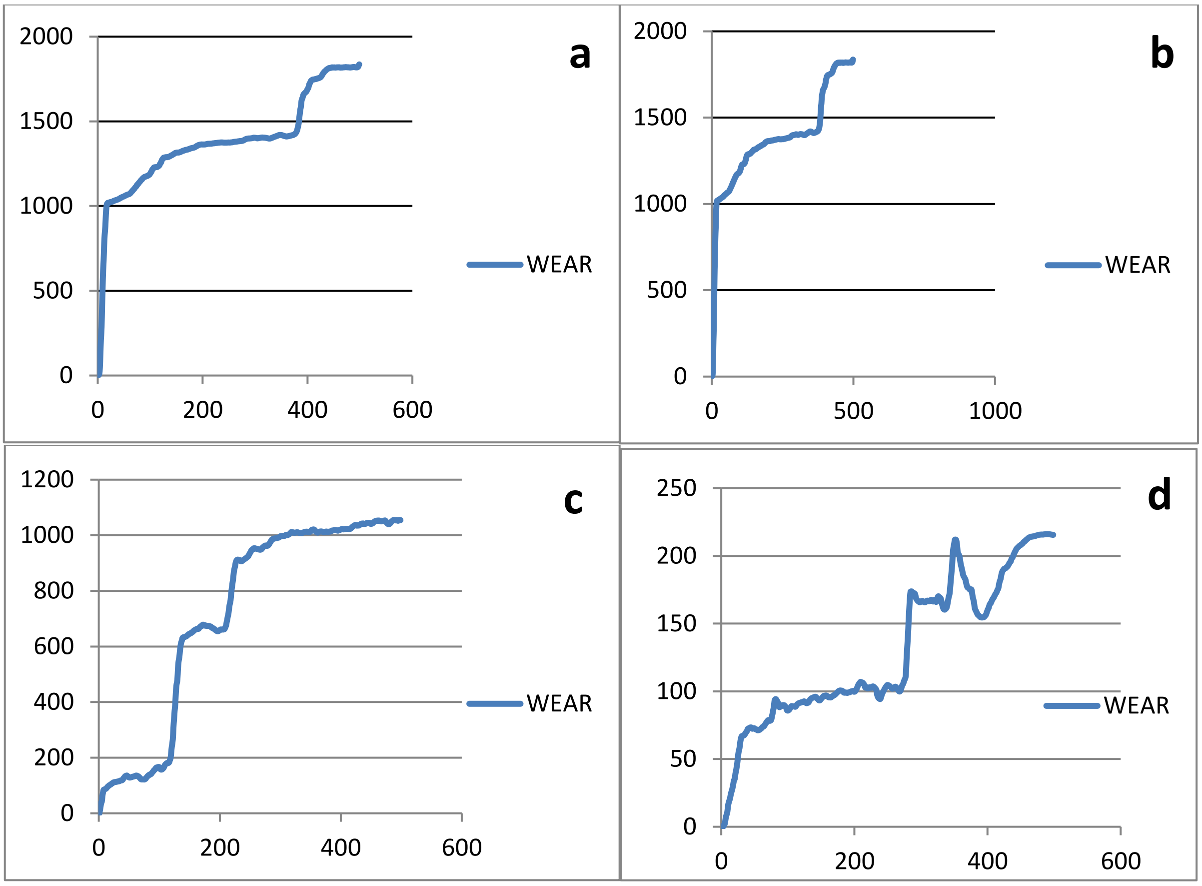


**Figure 7**. Time Vs Wear rate for sample a, b, c, and d.

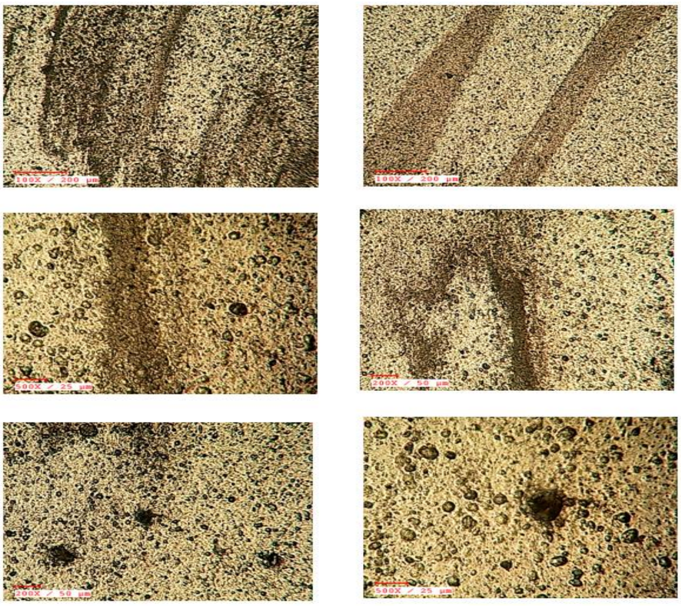

**Figure 8.** OM images of test plate 1(50% $Cu_2O$& 50% $Cr_3C_2$).

**Optical Microscope**

Microstructure of the FSP sample by the help of Optical microscope has been observed from TP-1 to T.P-3 5.5.1 FSP Plate TP 1 and shown in Figure 8. The TP-1 structure was largely homogeneous, with massive precipitates and partially broken flaws. During FSP, intense plastic deformation and heat input result in the dissolution of precipitates, the refinement of matrix grains, the closure of porosity, and the breakdown of coarse dendrites and second-phase particles, all of which contribute to the creation of a fine, homogeneous, and flawless structure shown in Figure 10. In this study, sound FSW butt joints from AA6061 specimens were acquired. This demonstrates the unique qualities of the FSW procedure. In FSW, plastic deformation and heat produced by tool spinning on AA6061 plates are used to weld the plates together. The plates are softened by the heat that is produced. This makes the substance flow easier.

The microstructure's optical micrographs exhibit notable variations in relation to both rotational and trip speeds. It can be argued that medium traveling speed rates resulted in increased heat input, which profoundly altered the microstructure below the surface, where little grains were visible. In this study, sound FSW butt joints from AA6061 specimens were acquired shown in figure 9. This demonstrates the unique qualities of the FSW procedure. In FSW, plastic deformation and heat produced by tool spinning on AA6061 plates are used to weld the plates together. The plates are softened by the heat that is produced. This makes the substance flow easier. Upper surface with a homogeneous distribution of 50% BN and 50% $Cu_2O$ particles. Both particles can be finely dispersed to reduce grain growth and produce ultrafine grain sizes. In this study, sound FSW butt joints from AA6061 specimens were acquired. This demonstrates the unique qualities of the FSW procedure shown in figure 10. In FSW, plastic deformation and heat produced by tool spinning on AA6061 plates are used to weld the plates together. The plates are softened by the heat that is produced. This makes the substance flow easier.

**Scanning Electron Microscope (SEM)**

The FSP sample's microstructure has been studied using a scanning electron microscope. The stir processing zone is primarily taken into account. The primary goal is to determine how changes in the different reinforcements that were used as input parameters affect the microstructure. A scanning electron microscope (SEM) test is a high-resolution imaging technique that uses a focused beam of electrons to produce detailed surface images of a sample. It's commonly used in materials science, biology, and other fields to examine the surface structure and composition of specimens at a very fine scale, often down to nanometres. SEM provides valuable information about surface topography, morphology, and elemental composition shown in figure 11. The relatively uniform distribution of copper oxide and chromium carbide in the dark zone, as shown by the TP-1 SEM analysis, verifies the presence of the aluminium alloy 6061. $Cu_2O$ and $Cr_3C_2$ precipitates agglomerated in the reinforcements due of the process speed. Both reinforcements were present in the coarse precipitates in the bright zone.

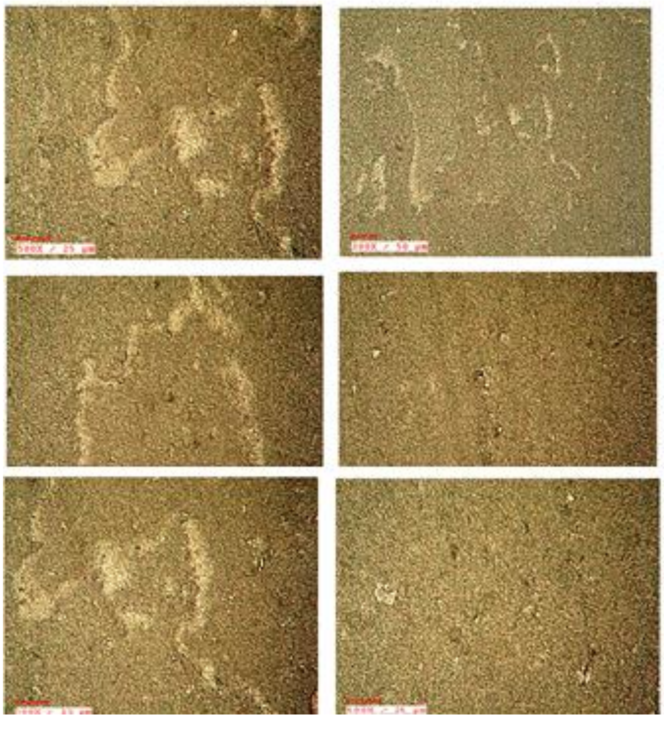

**Figure 9.** OM images of test plate 2 (50% $Cr_3C_2$ &50% BN).

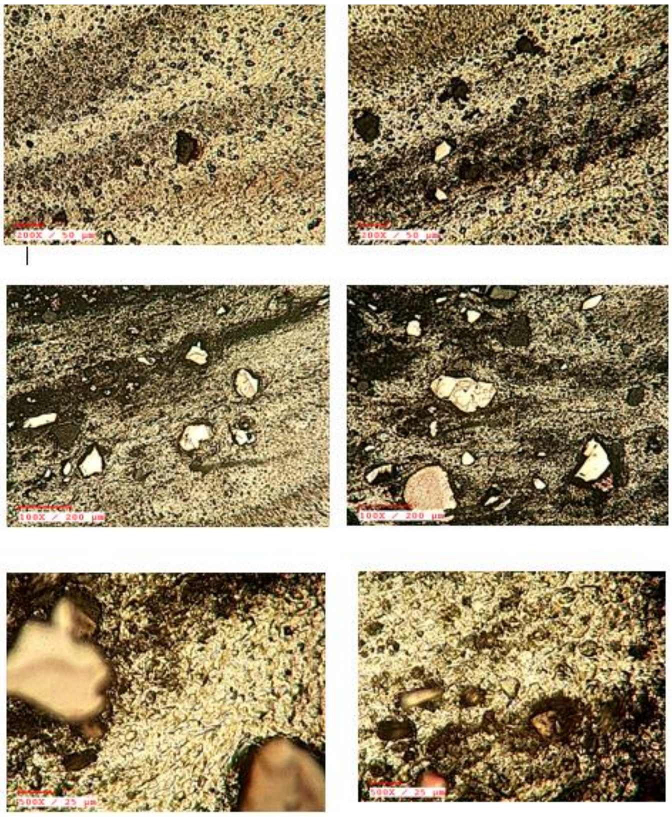

**Figure 10.** OM images of test plate 3 (50% BN &50%, $Cu_2O$).

A scanning electron microscope (SEM) test is a high-resolution imaging technique that uses a focused beam of electrons to produce detailed surface images of a sample. It's commonly used in materials science, biology, and other fields to examine the surface structure and composition of specimens at a very fine scale, often down to nanometres. SEM provides valuable information about surface topography, morphology, and elemental composition shown in Figure 8. Increased grain boundaries and dislocation density during dynamic recrystallization, which can serve as precipitate nucleation sites, also explain the precipitation behaviours shown by TP-2 SEM in the bright and dark areas of the stir zone. A scanning electron microscope (SEM) test is a high-resolution imaging technique that uses a focused beam of electrons to produce detailed surface images of a sample. It's commonly used in materials science, biology, and other fields to examine the surface structure and composition of specimens at a very fine scale, often down to nanometers. SEM provides valuable information about surface topography, morphology, and elemental composition shown in figure 8. The precipitation behaviours observed by TP-3 SEM analysis in the bright and dark portions of the stir zone can also be explained by the increased density of dislocations and grain boundaries during dynamic recrystallization, which can serve as precipitate nucleation sites.

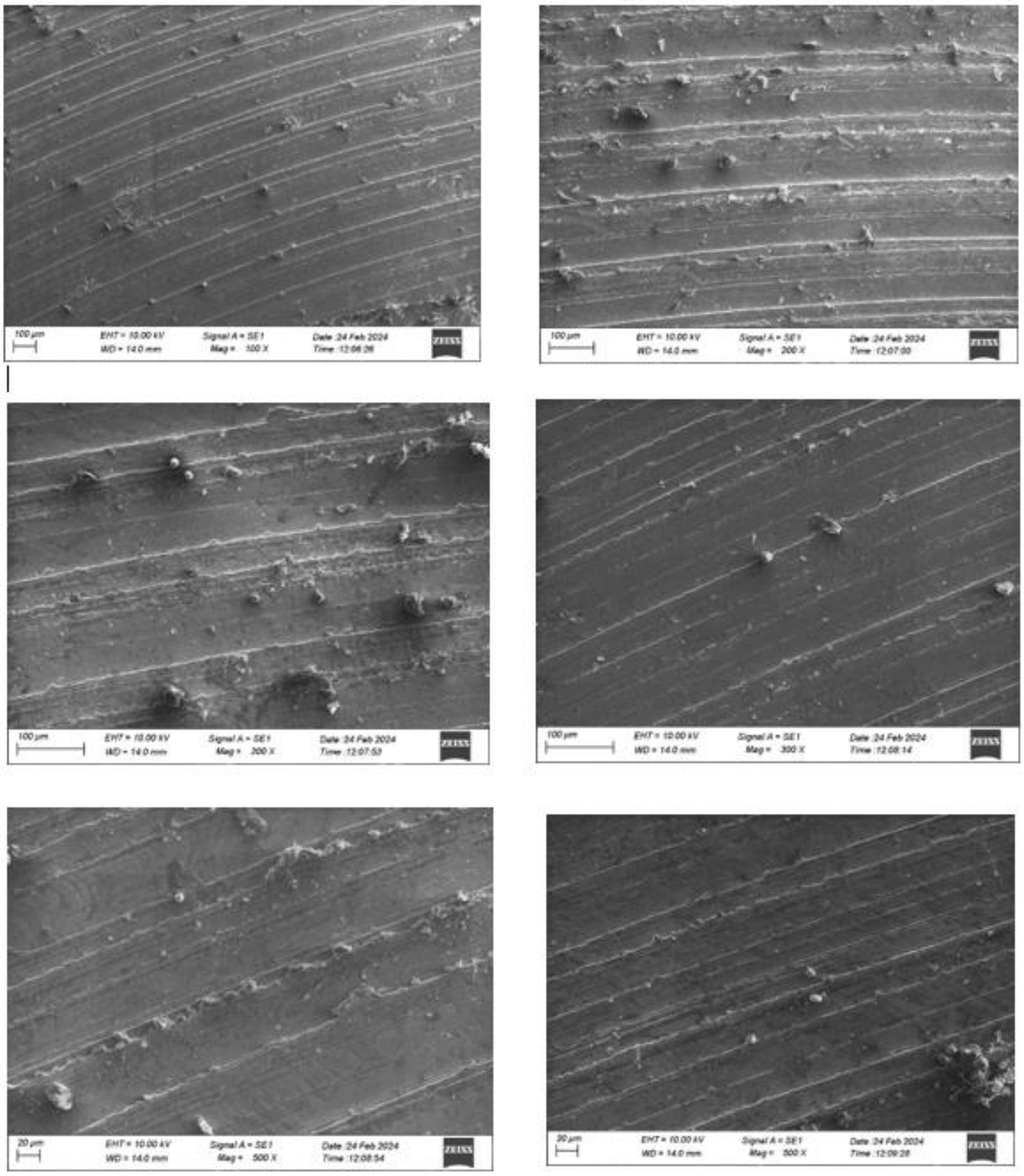

**Figure 11.** SEM images of test plate 2 (50%$Cr_3C_2$&50%BN).

## CONCLUSION

The distribution of the particles in the Al metal matrix with different reinforcement after a single FSP pass produced improved hardness and impact strength characteristics. Test Plate No. 2 (50% Chromium carbide 50% Boron Nitride), which was identified during the hardness experiment, increases the maximum surface hardness. Test Plate 2 consequently displays a higher hardness value in the FSP process. The maximum impact load was achieved test plate of the FSP T2- 36 J and then followed by test plate no -1 -16J with 50% $Cu_2O$& 50% $Cr_3C_2$. During the analysis the wear had been found the minimum wear rate occurred on the Ratio 3 - 50% BN &50% $Cu_2O$ (Combination of boron nitride and copper oxide) is obtained very low wear rate. Traveling at faster speeds generated more heat input, which profoundly altered the microstructure beneath the surface, where minuscule grains were visible, according to the microstructure SEM analysis medium. From the upper surface of the optical microscope, where the particles of $Cu_2O$ are uniformly dispersed and contain 50% h-BN. Both particles can be finely dispersed to produce an ultrafine grain size and restrict grain growth.

## REFERENCES

1. Salih, O.S., Ou, H., Sun, W. and McCartney, D. G. (2015) A review of friction stir welding of aluminium matrix composites. *Materials & Design*, **86,** 61–71.

2. Gangil, N., Siddiquee, A. N. and Maheshwari, S. (2017) Aluminium based in-situ composite fabrication through friction stir processing: A

review. *Journal of Alloys and Compounds*, **715**, 91–104.

3. Preethi, V. and Das, A. D. (2021) Optimization of friction stir welding parameters for better hardness in weld nugget of hybrid aluminium composite. *Materials Today: Proceedings*, **37**, 723–727.

4. Elatharasan, G. and Kumar, V. S. (2013) An experimental analysis and optimization of process parameter on friction stir welding of AA 6061-T6 aluminum alloy using RSM. *Procedia Engineering*, **64**, 1227–1234.

5. Arokiasamy, S. and Anand Ronald, B. (2017) Experimental investigations on the enhancement of mechanical properties of magnesium-based hybrid metal matrix composites through friction stir processing. *The International Journal of Advanced Manufacturing Technology*, **93**, 493–503.

6. Saravanakumar, S., Gopalakrishnan, S., Kalaiselvan, K. and Prakash, K. B. (2021) Microstructure and mechanical properties of Cu/RHA composites fabricated by friction stir processing. *Materials Today: Proceedings*, **45**, 879–883.

7. Yaknesh, S., Tharwan, M., Saminathan, R., Rajamurugu, N., Prakash, K. B., Ankit, Pasupathi, M. K., Sarojwal, A. and Gebreyohannes, D. T. (2022) Mechanical and microstructural investigation on AZ91B Mg alloys with tool tilt variation by friction stir welding. *Advances in Materials Science and Engineering*, **2022 (1)**, 8311413.

8. Saravanakumar, S., Prakash, K. B., Chandru, M. and Durairaj, M. (2016) Characterization of Copper Matrix Composite Reinforced with Aluminium Nitrate using Friction Stir Processing Techniques. *Iciems*, **1**, 58–62.

9. Peter, P. I. and Adekunle, A. A. (2020) A review of ceramic/bio-based hybrid reinforced aluminium matrix composites. *Cogent Engineering*, **7(1)**, 1727167.

10. Babu, B. S., Prathap, P., Balaji, T., Gowtham, D., Adi, S. S., Divakar, R. and Ravichandran, S. (2020) Studies on mechanical properties of aluminum based hybrid metal matrix composites. *Materials Today: Proceedings*, **33**, 1144–1148.

11. Rao, C. M. and Rao, K. M. (2017) Studies on Friction Stir Welding of Aluminium Alloys 6061-To-6061 Similar Metals. *International Journal of Mechanical Engineering and Technology*, **8(1)**.

12. Bourkhani, R. D., Eivani, A. R. and Nateghi, H. R. (2019) Through-thickness inhomogeneity in microstructure and tensile properties and tribological performance of friction stir processed AA1050-Al2O3 nanocomposite. *Composites Part B: Engineering*, **174**, 107061.

13. Khoshaim, A. B., Moustafa, E. B., Bafakeeh, O. T. and Elsheikh, A. H. (2021) An optimized multilayer perceptrons model using grey wolf optimizer to predict mechanical and micro-structural properties of friction stir processed aluminum alloy reinforced by nanoparticles. *Coatings*, **11(12)**, 1476.

14. Bourkhani, R. D., Eivani, A. R., Nateghi, H. R. and Jafarian, H. R. (2020) Effects of pin diameter and number of cycles on microstructure and tensile properties of friction stir fabricated AA1050-Al2O3 nanocomposite. *Journal of Materials Research and Technology*, **9(3)**, 4506–4517.

15. Ammouri, A. H., Kridli, G., Ayoub, G. and Hamade, R. F. (2015) Relating grain size to the Zener–Hollomon parameter for twin-roll-cast AZ31B alloy refined by friction stir processing. *Journal of Materials Processing Technology*, **222**, 301–306.

16. Dwivedi, S. P., Sharma, S., Li, C., Zhang, Y., Kumar, A., Singh, R., Eldin, S. M. and Abbas, M. (2023) Effect of nano-TiO2 particles addition on dissimilar AA2024 and AA2014 based composite developed by friction stir process technique. *Journal of Materials Research and Technology*, **26**, 1872–1881.

17. Khodabakhshi, F. and Gerlich, A. P. (2020) On the correlation between indentation hardness and tensile strength in friction stir processed materials. *Materials Science and Engineering: A*, **789**, 139682.

18. Djouider, F., Alhawsawi, A., Elmoujarkach, E., Banoqitah, E., Alharazi, M. and Moustafa, E. B. (2023) The role of friction stir processing parameters and hybrid ZrC/WC reinforcement particles in improving the surface composite dissimilar matrix's dynamic behavior and micro-structure refinement. *Coatings*, **13(8)**, 1393.

19. Mosleh, A. O., Yakovtseva, O. A., Kishchik, A. A., Kotov, A. D., Moustafa, E. B. and Mikhaylovskaya, A. V. (2023) Effect of coarse eutectic-originated particles on the microstructure and properties of the friction stir-processed Al-Mg-Zr-Sc-based alloys. *Jom*, **75(8)**, 2989–3000.

20. Moustafa, E. B., Mikhaylovskaya, A. V., Taha, M. A. and Mosleh, A. O. (2022) Improvement of the microstructure and mechanical properties by hybridizing the surface of AA7075 by hexagonal boron nitride with carbide particles using the FSP process. *Journal of Materials Research and Technology*, **17**, 1986–-1999.

21. Ghandourah, E. I., Moustafa, E. B., Hussein, H. and Mosleh, A. O. (2021) The effect of incorporating ceramic particles with different morphologies on the microstructure, mechanical and tribological behavior of hybrid TaC_BN/AA 2024 nanocomposites. *Coatings*, **11(12)**, 1560.

22. Kulitskiy, V., Malopheyev, S., Mironov, S. and Kaibyshev, R. (2016) Grain refinement in an Al-Mg-Sc alloy: Equal channel angular pressing versus friction-stir processing. *Materials Science and Engineering: A*, **674**, 480–490.

23. Verma, S., Msomi, V., Mabuwa, S., Merdji, A., Misra, J. P., Batra, U. and Sharma, S. (2022) Machine learning application for evaluating the friction stir processing behavior of dissimilar aluminium alloys joint. *Proceedings of the Institution of Mechanical Engineers, Part L: Journal of Materials: Design and Applications*, **236(3)**, 633–646.

24. Rabe, P., Reisgen, U. and Schiebahn, A. (2023) Non-destructive evaluation of the friction stir welding process, generalizing a deep neural defect detection network to identify internal weld defects across different aluminum alloys. *Welding in the World*, **67(3)**, 549–560.

25. Saravanakumar, S., Kalaiselvan, K., Prakash, K. B., Parkunam, M., Niranjan, S., Dharanish, N. and Akash, R. (2022) Mechanical behaviour and microstructure analysis of aluminium 2024 and 5052 using friction stir welding. *Materials Today: Proceedings*, **69**, 1437–1441.

26. Yaknesh, S., Rajamurugu, N., Prakash, K. B., Saleel, C. A., Rajendran, P., Lee, I. and Arputharaj, B. S. (2024) A critical review on the performance and microstructural characteristics of materials fabricated through friction stir additive methods and deposition techniques. *Journal of Materials Research and Technology*.

27. Saravanakumar, S., Prakash, K. B., Dinesh, D., Kumar, P. M., Fouad, Y., Soudagar, M. E. M., Ali, M. M. and Bashir, M. N. (2024) Optimizing friction stir processing parameters for aluminium alloy 2024 reinforced with SiC particles: A taguchi approach of investigation. *Journal of Materials Research and Technology*, **30**, 4847–4855.

28. Yaknesh, S., Rajamurugu, N., Babu, P. K., Subramaniyan, S., Khan, S. A., Saleel, C. A., Nur-E-Alam, M. and Soudagar, M. E. M. (2024) A technical perspective on integrating artificial intelligence to solid-state welding. *The International Journal of Advanced Manufacturing Technology*, **132(9)**, 4223–4248.

29. Yaknesh, S., Tharwan, M., Saminathan, R., Rajamurugu, N., Prakash, K. B., Ankit, Pasupathi, M. K., Sarojwal, A. and Gebreyohannes, D. T. (2022) Mechanical and microstructural investigation on AZ91B Mg alloys with tool tilt variation by friction stir welding. *Advances in Materials Science and Engineering*, **2022(1)**, 8311413.

30. Kadaganchi, R., Gankidi, M. R. and Gokhale, H. (2015) Optimization of process parameters of aluminum alloy AA 2014-T6 friction stir welds by response surface methodology. *Defence Technology*, **11(3),** 209–219.

31. Vijayakumar, S., Anitha, S., Arivazhagan, R., Hailu, A. D., Rao, T. J. and Pydi, H. P. (2022) Wear investigation of aluminum alloy surface layers fabricated through friction stir welding method. *Advances in Materials Science and Engineering*, **2022(1)**, 4120145.

32. Shao, C., Zhao, S., Wang, X., Zhu, Y., Zhang, Z. and Ritchie, R. O. (2019) Architecture of high-strength aluminum–matrix composites processed by a novel microcasting technique. *NPG Asia Materials*, **11(1)**, 69.

33. Arul, M., Subramaniyan, C., Sakthivelmurugan, E. And Sureshkumar, M. (2024) Optimising mechanical properties of epoxy matrix hybrid composites through sic filler integration and fiber reinforcement: *The Taguchi Approach. Cellulose Chemistry & Technology*, **58**.

34. Subramaniyan, C., Prakash, S. V., Bhuvanesh, N., Kalidasan, B. and Amarkarthik, A. (2021) Study based on the reduction of lot time by implementing set production and FMS in the traditional batch production system. *Materials Today: Proceedings*, **45**, 502–506.